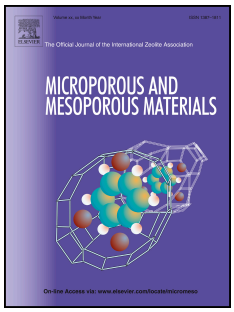

Tartrazine removal by ZnO nanoparticles and a zeolite-ZnO nanoparticles composite and the phytotoxicity of ZnO nanoparticles

A. Alcantara-Cobos, E. Gutiérrez-Segura, M. Solache-Ríos, A. Amaya-Chávez, D.A. Solís-Casados

PII: S1387-1811(20)30215-8

DOI: https://doi.org/10.1016/j.micromeso.2020.110212

Reference: MICMAT 110212

To appear in: *Microporous and Mesoporous Materials*

Received Date: 6 March 2020

Revised Date: 27 March 2020

Accepted Date: 30 March 2020

Please cite this article as: A. Alcantara-Cobos, E. Gutiérrez-Segura, M. Solache-Ríos, A. Amaya-Chávez, D.A. Solís-Casados, Tartrazine removal by ZnO nanoparticles and a zeolite-ZnO nanoparticles composite and the phytotoxicity of ZnO nanoparticles, *Microporous and Mesoporous Materials* (2020), doi: https://doi.org/10.1016/j.micromeso.2020.110212.

Credit author statement

A. Alcantara-Cobos: Investigation, formal analysis. E. Gutiérrez-Segura: Supervision, Conceptualization, Metodology. M. Solache-Ríos: Supervision, Writing- Reviewing and Editing. A. Amaya-Chávez: Resources, formal analysis. D.A. Solís-Casados: Resources, formal analysis.

,

Graphical abstract

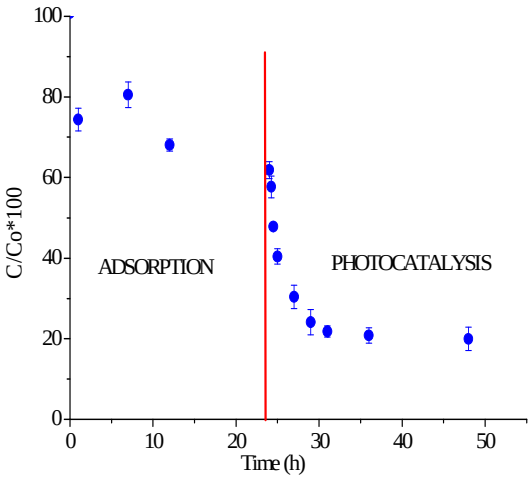

Tartrazine removal by ZnO nanoparticles and a zeolite-ZnO nanoparticles composite and the phytotoxicity of ZnO nanoparticles.

A. Alcantara-Cobos[1], E. Gutiérrez-Segura[1], M. Solache-Ríos[2]*, A. Amaya-Chávez[1], D.A. Solís-Casados[3]

[1] Facultad de Química, Universidad Autónoma del Estado de México, Paseo Colón y Tollocan s/n., C.P. 50000 Toluca, Estado de México, Mexico.

[2] Instituto Nacional de Investigaciones Nucleares, Departamento de Química. Carretera México-Toluca S/N La Marquesa, Ocoyoacac, México C. P. 52750.

[3] Centro Conjunto de Investigación en Química Sustentable UAEM-UNAM, Carretera Toluca, Atlacomulco Km 14.5, Unidad San Cayetano, Toluca, Estado de México, Mexico.

Abstract

ZnO nanoparticles (nanZnO) and a zeolite-ZnO nanoparticles composite (Ze-nanZnO) were prepared and characterized. These materials were used for the removal of tartrazine from aqueous solutions by an adsorption-photocatalysis coupled process.

The adsorption using nanZnO showed a rapid decrease of the concentration of tartrazine and the adsorption by using the composite Ze-nanZnO was slower. The degradation of tartrazine by using both materials in the presence of ultraviolet light seems to be a highly efficient process for both materials, 87 and 81% degradation were observed for nanZnO and Ze-

*Corresponding author. marcos.solache@inin.gob.mx, Tel.: +52 5553297200x2262; fax:+525553297301

nanZnO respectively, although the first material seems to be more efficient than the second, this first material is difficult to remove from the aqueous solution after the process. The mineralization was monitored by measuring the total organic carbon at different contact and irradiations times. The degradation of the dye was high between 85 and 90 %, higher degradation was observed using Ze-nanZnO as catalyst than nanZnO.
"Lactuca sativa" species suffer "low toxicity" when they are in contact with solutions containing the dye and solutions that were in contact with nanZnO

Keywords

ZnO nanoparticles; Tartrazine; Phytotoxicity; Adsorption; Photocatalysis.

1. Introduction

The dyes are important contaminants from the textile, food, paper, paint, pharmaceutical industries, among others, since in many cases, they are discharged directly to the effluents, causing environmental and aesthetic pollution [1]. They are classified as anionic (azoic, acid, direct and reactive dyes), cationic (basic dyes), and nonionic (disperse dyes) according to their dissociation in aqueous medium [2]. Azo dyes are more than a half of the dye species in textile wastewater [3]; its treatment is very difficult because the sulphonic acid groups makes the dyes polar and more soluble in water. Therefore, these dyes are not easily adsorbed on an activated carbon with nonpolar surface. Then, dyes should be degraded and their degradation products (aromatic amines) removed by adsorption [4]. Tartrazine dye is a typical azo dye, commonly used as an additive in the food industry; such as, moisturizing and energizing beverages, bread, chips, sweet ice cream, chewing gums, gelatins and yoghurt, in addition it is used in capsule in the pharmaceutical industry [5].

Some reports indicate that tartrazine can cause allergy and asthma, hypersensitivity, mutagenic and carcinogenic effects, skin eczema and immunosuppressive effects [6]. In general, there are several methods to remove dyes from water, such as biological, membranes, coagulation, adsorption and photocatalysis, among others processes [1]. Adsorption is one of the most promising methods, since it is efficient, simple to design, economical and does not have toxic effects [7]. Various adsorbents have been developed for the removal of dyes from wastewater with favorable results, among them zeolites [8]. Photocatalysts are semiconductors, which respond to a light stimulus with an energy equal or higher than their band gap interval, producing hollow-electron pairs. Some of these charges migrate to the surface of the crystal where they participate in oxide-reduction reactions of the adsorbed species, like mineralization (carbon dioxide and water) of the polluting organic molecules [9,10]. TiO_2, ZnO, Fe_2O_3 or V_2O_5 are considered to be the most important photocatalysts in the environmental field and ZnO is an important direct broadband semiconductor II-VI with a band interval of 3.2 eV [11]. Recently ZnO of nanometric size has received important attention due to its low cost and high photochemical activity, due to its high surface area derived from the particle size, this material was used in the degradation of the rhodamine dyes type with high efficiency [12]. The removal of AB92 azo dye was achieved by using ZnO/Mordenita photocatalyst [13]. 80% photodegradation of methylene blue by ZnO in 180 minutes was also reported [14]. On the other hand, it is important to consider the toxicity of both the nanoparticles and the degradation products of the dyes. In America, the presence of ZnO nanoparticles has not been reported, while in Europe, concentrations of 0.01 g L^{-1} have been reported in surface water and 0.432 g L^{-1} in wastewater, specifically in Switzerland, and in other effluents a concentration of 0.441 g L^{-1} has been detected [15]. A study of ZnO nanoparticles in

contact with *Prosopis juliflora-velutina* increased the antioxidant activity of catalase (CAT) and ascorbate peroxidase (APOX), mainly in the root where the highest absorption of nanoparticles was observed [16]. On the other hand, the effect of ZnO nanoparticles of size 17.4±4.9 nm on maize (*Zea mays Leaf*) and cabbage (*Brassica oleraceae var. Capitata L.*) was negative, the maize cells of the roots showed structural damage but did not affect the germination in cabbage (the elongation of the root did not change) [17]. The toxic effects of nanoparticles of ZnO and Zn^{2+} were also evaluated in *Lactuca sativa*, with concentration of 2000 mg L^{-1}, the presence of these materials reduces the germination and growth rate of the plant [18].

In a previous paper [19], both nanZnO and Ze-nanZnO were used as adsorbents for the removal of tartrazine from aqueous solutions and the adsorption was higher for the nanoparticles of ZnO than the composite. Therefore, the purpose of this research was to use a hybrid photocatalysts formed by nanometric ZnO deposited on a zeolite, this composite can combine the adsorption and photocatalytic degradation processes on the removal of tartrazine dye from aqueous solutions and to compare the degradation behavior with nanZnO. Furthermore the toxic effects of the ZnO nanoparticles on the seed germination of lettuce (*Lactuca sativa*) were studied.

2. Experimental

2.1. Materials

The zeolite from the Etla zone in the State of Oaxaca, Mexico was crushed and sieved, the particles between 0.85 and 0.60 mm were selected. The $(CH_3COO)_2Zn{\cdot}2H_2O$ and NaOH were from Merck and tartrazine (CAS 1934-21-0) was Sensient Food Colors brand.

2.2. Samples preparation

ZnO nanoparticles-zeolite composite was prepared as reported elsewhere [19] by the chemical precipitation. Clinoptilolite type zeolite was left in contact with a zinc acetate solution, then a NaOH solution was added (1 mL/min), the mixture was stirred for 2 hours and refluxed. The precipitate was washed with deionized water and ethanol, dried at 80°C and calcined at 300°C to obtain the ZnO nanoparticles-zeolite composite (Ze-nanZnO). The ZnO nanoparticles (nanZnO) were prepared in the same way without adding the zeolitic material.

2.3. Characterization

The ZnO nanoparticles (nanZnO) and the zeolite-ZnO nanoparticles composite (Ze-nanZnO) were analyzed by powder X-ray diffraction patterns (XRD), using a D500 diffractometer with radiation of Kα line of Cu anode (λ = 1.54 Å) in the range of 20 ° <2Θ <90 with a speed of 2°/ min. The samples were analyzed by using a scanning electron microscope (JEOL JSM-5900-LD) coupled to a Zonda EDS DX-4. The TEM images of the ZnO nanoparticle samples were obtained by using a transmission electron microscope (JEOL-2010). The band gaps energy of the nanZnO and Ze-nanZnO materials were determined from the UV-Vis (DRS) spectra by using the Kubelka-Munk function, the spectra were acquired in the diffuse reflectance mode using a sphere of integration in a Perkin Elmer Lambda 35 spectrophotometer. The characteristic binding vibrations were determined by infrared spectroscopy (IR), with a Bruker model TENSOR 27 equipped with a total attenuated reflection accessory (ATR), in the range of 400-4000 cm^{-1} with a resolution of 3 cm^{-1} and 300 scanning. The nanZnO material was placed in colloidal

suspension and sonicated for 15 minutes to disperse the sample and then the spectrum was obtained in diffuse reflectance mode (DRS), in a range of 250 - 500 nm using a UV / Vis Genesys 10s spectrophotometer. The total organic carbon (TOC) was measured in the samples (Filters Millipore-Miliex-GN Nylon 0.2 mm) by using a Shimadzu-5050A TOC analyzer.

2.4. Evaluation of the adsorption photocatalysis process

100 mg of nanZnO or Ze-nanZnO materials, used as photocatalyst, were left in contact different times with 10 mL of the tartrazine dye solution with a concentration of 10 mg/L, then the mixtures were irradiated with ultraviolet light using a Tecno Lite lamp that radiates energy of 3.35 eV and a power of 20 W, the degradation after 15, 30 min, 1, 3, 5, 7, 12, 14 h was evaluated by measuring the absorbance at λmax = 426.7 nm in the remaining solutions by using an UV-Vis Genesis 10S spectrophotometer.

The degradation percentage was calculated by using the Equation 1:

$$\%\, Degradation = \frac{(C_i - C_t)}{C_i} * 100 \qquad \text{Equation 1}$$

where:

C_i = Initial concentration of the dye in solution (mg L^{-1})

C_t = Concentration of the dye in solution at time t (mg L^{-1})

Mineralization of tartrazine dye was monitored by measuring the total organic carbon (TOC) in each sample by using a Shimadzu VCSN/CPN Model TOC analyzer. All plots were generated by the help of Origin Pro 8.

2.5. Bioassay on the species "*Lactuca sativa*"

Lactuca sativa (seed germination > 90 %) were used in the current study. This bioassay was performed using the remaining aqueous solution from the treatments of the dye solutions with nanZnO and following the US EPA procedure (1996) [20, 21], germination of seeds for acute toxicity and elongation of hypocotyl and radicle for toxicity subacute. The toxicity is related to the solubility in water of the contaminant and reflects the behavior of a contaminant, the high risk of dispersion as well as the solubilization and bioavailability of the contaminant in the environment. 20 seeds of *Lactuca sativa* were placed on filter paper in 90 mm diameter Petri dishes, four milliliters of the following samples were deposited in each recipient; control (-): distilled water, control (+): 10 mg/L of tartrazine solution, nanoparticles in aqueous medium: remaining aqueous solutions after treatments and diluted (100, 75, 50, 25 and 12.5%), subsequently they were placed in an incubator (40050-IP-20 Memmert, Bundesrepublik Deutschland, Germany) for 120 h at 22 ± 0.1 °C, all experiments were done in triplicate. Finally, seeds that germinated were counted, and the lengths of the radicles and the hypocotyls of the germinated seeds were measured. The data were used to establish two toxicity indexes:

Seed germination (SG) was calculated by using Equation 2: In statistical terms, it represents the normalized residual percentage of seed germination after the experiment.

$$SG = \frac{(Germ_{sample(i)} - Germ_{control})}{Germ_{control}} \qquad \text{Equation 2}$$

where:

$Germ_{sample(i)}$= The average number of seeds germinated for each solution (i)

$Germ_{control}$= The average number of seeds germinated for the control (-)

Root and hypocotyl elongation (RE and HE) were calculated by Equation 3 and 4 respectively: In statistical terms, they represent the normalized residual elongation of the radicle and hypocotyl of the seeds germinated after the experiments.

$$RE = \frac{(Relong_{sample(i)} - Relong_{control})}{Relong_{control}}$$ Equation 3

$$HE = \frac{(Helong_{sample(i)} - Helong_{control})}{Helong_{control}}$$ Equation 4

where

$Relong_{sample(i)}$= Average length of the radicle for each solution (mm)

$Helong_{sample(i)}$= Average hypocotyl length for each solution (mm)

$Relong_{control}$= Average length of the radicle for the negative control (mm)

$Helong_{control}$= Average hypocotyl length for the negative control (mm)

2.6. Statistical analysis

The elongation results are presented as mean ± standard error of the mean values (SE) of the eight independent treatments. Differences between elongation means were evaluated for significance by one-way analysis of variance (ANOVA) and Dunnet test for multiple comparisons using Minitab 17.2.1 statistical software (USA). Differences were considered statistically significant when $p < 0.05$.

3. Results and discussion

3.1. Characterization

3.1.1. X-Ray diffraction analysis

X-ray diffraction patterns of nanZnO obtained by chemical precipitation is shown in Fig. 1(a), reflection peaks correspond to the crystal structure of ZnO in hexagonal wurzite phase for nanZnO according to the JCPDS 36-1451 as reported elsewhere [19]. The diffraction patterns of Ze-nanZnO is shown in Fig. 1(b), the structure of zeolite corresponds to clinoptilolite [JCPDS No. 39-1383] and ZnO to the wurzite phase. In addition, other phases are present, such as quartz and heulandite zeolite, clinoptilolite is associated with the series of zeolite tectonic-silicate minerals named heulandite with a varying Si/Al ratio of 4.0 to 5.3, they have been describe elsewhere [22]. The average size of the nanZnO particles was around 42.7 nm and the distribution of the size of the nanoparticles was similar as reported elsewhere [19]. The average size was determined by using the width at the mean height of the most intense peak of the diffractogram and the Scherrer equation (Equation 5). A size of 28.28 nm was reported elsewhere [19].

$$d_c = \frac{k\lambda}{\beta cos\Theta} \qquad \text{Equation 5}$$

3.1.2. Scanning electron microscopy and elemental analysis by X-rays dispersive energy (EDS).

Fig. 2 (a-d) shows the images of nanZnO and Ze-nanZnO before and after the coupled adsorption-photocatalysis process, the images show grains of heterogeneous morphology and different sizes and shapes for both materials and the presence of smaller particles agglomerated on the surface of the material (2-10 μm). In general, there are not any important morphological differences in the material after the deposition process of the ZnO nanoparticles on the surface of the zeolite (Fig. 2(c)). The surface of the materials after the

treatment of the aqueous solutions of the dye are shown in Figs. 2(b) and 2(d), a non-uniform layer on the surface of the materials is observed.

The composition percentage of the synthesized nanoparticles was evaluated by EDS analysis. The EDS patterns of the nanZnO and Ze-nanZnO show that the content of zinc was 76.4 and 9.3%, respectively. Other chemical elements (Al, Si, and K) are also present in the Ze-nanZnO sample, they correspond to the natural zeolite and may be important in the removal processes. It is important to note that significant amounts of carbon (26.2±6.7 and 21.5±2.5 in nanZnO and Ze-nanZnO respectively) appear in the materials after the removal process, this indicates that a part of the dye is fixed on the surface of the material by adsorption and other part is mineralized by the photocatalysis process.

3.1.3. Transmission Electron Microscopy (TEM)

In many cases, the behavior of the nanZnO and Ze-nanZnO depends on their shape and size, the nanZnO material was characterized by TEM in order to have a more accurate estimation of the size and shape of the ZnO particles. The corresponding images are shown in the Fig. 2(e-f), the main ZnO particles have a quasi-spherical shape and an average size of 68 ± 6.74 nm. However, these particles tend to agglomerate, which can reduce their efficiency as adsorbents and catalysts (Fig. 2(f)). The mean size is similar to the one reported for ZnO nanoparticles (75 nm) obtained by suspension method in basic medium [23]. ZnO nanoparticles synthesized by poly acrylamide pyrolysis showed a mean diameter of 58 nm and demonstrated that these nanoparticles usually tend to aggregate at high calcination temperature [24].

3.1.4. UV-Vis Spectroscopy

Fig. 3 (a-b) shows the adsorption spectra of nanZnO in suspension and commercial ZnO (Baker) in bulk, both materials show a characteristic absorption edge of the ZnO semiconductor located below 400 nm. Adsorption is displaced to the blue zone of the electromagnetic spectrum compared to commercial zinc oxide in bulk, this effect is attributed to the particle size, since it is in the quantum regime. The average particle radius of nanoparticles in colloidal suspension can be determined by using the effective mass model in eV and the Equation 6 [13]:

$$(E)^{\phi} = E_g^{bulk} + \frac{h^2}{2er^2}\left(\frac{1}{m_e^{\phi} m_0} + \frac{1}{m_h^{\phi} m_0}\right) - \frac{1.8e}{4\pi\varepsilon\varepsilon_0 r} - \frac{0.124e^3}{h^2(\pi\varepsilon\varepsilon_0)^2}\left(\frac{1}{m_e^{\phi} m_0} + \frac{1}{m_h^{\phi} m_0}\right)^{-1} \quad \text{Equation 6}$$

where E_g^{bulk} bulk is the band gap energy of ZnO in bulk (3.2 eV), h is Planck's constant, r is the radius of the particle, m_e^{ϕ} and m_h^{ϕ} are the effective mass of the electron and gap, respectively, m_0 is the mass of the free electron, e is the charge of the electron, ε_0 is the permissiveness of the free space. Using the effective mass model, a particle radius of 32 nm was determined for nanZnO. According to the calculations, the average crystallite size of nanZnO was lower than the value obtained by TEM characterization.

3.1.5. Analysis of nanZnO and Ze-nanZnO by UV-Vis spectroscopy in diffuse reflectance mode (Kubelka-Munk function)

The UV-Vis spectra of nanZnO and Ze-nanZnO are shown in Fig. 3 (c-d). The absorbance spectra (Fig. 3(c)) evidenced the characteristic reflectance of nanZnO located between 375 and 400 nm. UV-Vis spectral data in the diffuse reflectance mode were transformed to the Kubelka-Munk function (F^2) to separate the extent of light absorption from scattering [25].

The values of band gap of nanZnO and Ze-nanZnO are found to be 3.21 and 3.23 eV, respectively (Fig. 3(d)), these values are similar to other reported elsewhere [25,26]. Values similar of band gap between nanZnO and Ze-ZnO composite indicate that the cations from the zeolite were exchanged by Zn^{2+}, and their presence enhances the photocatalytic activity due to the enhanced formation of the photo-electrons and photo-holes [9].

3.1.6. Infrared spectroscopy (FT-IR)

The FT-IR spectra of nanZnO and Ze-nanZnO composite are shown in the Fig. 4(a-b). Vibration bands at 3349 and 1648 cm^{-1} are assigned to O-H stretching due to H_2O located within the pores of both nanZnO and zeolite. Bands between 400 and 500 cm^{-1} are assigned to Si-O-Si bending vibrations [27]. Comparing the FT-IR spectra of the nanZnO and Ze-nanZnO composite shows that, the small decrease in the intensity, widening and displacement of the peaks between 400 and 500 cm^{-1} are due to the presence of nanZnO on the porous system of crystalline structure of the zeolite; this behavior has been observed elsewhere [28]. On the other hand the IR spectra of the materials after the adsorption process show bands at 1176, 1124, 1035, 1006 cm^{-1}, which are related to C_6H_5- N = N-, -C-C-, -C = C- respectively, which overlap and they form a single peak between 900 and 1400 cm^{-1}. Between 500 and 700 cm^{-1} there is an increase in the intensity of the peaks that are related to C_6H_5- SO_2-, -CCO, S = O, R-SO_3-Na^+ and groups C_6H_5-, R-C_6H_4-R_1. Typical bands related to -N = N, are observed at about 1000 and 500 cm^{-1} [29].

3.2. Evaluation of the adsorption-photocatalysis coupled process

The characteristic absorption peaks of the tartrazine were used to monitor its adsorption and degradation over time. The successive decrease of the peak intensity of the most representative peak of the dye molecule during the adsorption and degradation processes indicates its removal from the aqueous solution. Tartrazine is a cationic dye, the most intense peak is at 426.7 nm (Fig. 5), in the first hours of the process, a large amount of the dye is removed, and this is because initially more active sites are available for the adsorption of dye molecules. It was also observed that the degradation of the dye was intense at the beginning of irradiation with direct ultraviolet light and the equilibrium was reached in almost 24 hours. After 12 hours of contact, a shoulder was observed at 370 nm, which may indicate the photodegradation reaction generates byproducts.

Fig. 6(a, b) shows the results on the adsorption and photocatalytic degradation of tartrazine in solution by using nanZnO and Ze-nanZnO, respectively. The adsorption using nanZnO showed a rapid decrease of the concentration of tartrazine and the adsorption with the composite Ze-nanZnO was slower and the equilibrium was reached in 24 hours. The degradation of tartrazine by using nanZnO and Ze-nanZnO in the presence of ultraviolet light after adsorption seems to be a highly efficient process for the two materials, 87 and 81% of degradation were observed for nanZnO and Ze-nanZnO respectively, the shape and the size of the particles of the materials are important in this kind of processes. Although the first material seems to be more efficient than the second, this first material is difficult to remove from the aqueous solution after the process.

3.3 Total organic carbon (TOC)

The total degradation of a dye can be determined by quantifying the total organic carbon (TOC) present in the treated remaining aqueous solutions. The mineralization of the

organic compound produces CO_2 and H_2O, the degradation kinetics of the dye was monitored by measuring the total organic carbon at different contact and irradiations times (Fig. 7). The degradation of the dye was high (85 and 90 %), it is important to note that the degradation process by using the nanZnO material is faster than Ze-nanZnO, however higher degradation was observed using the last material.

3.4. Bioassay on the species "*Lactuca sativa"*

Zn is an essential micronutrient that plays a vital role in maintaining cell membrane integrity and cell elongation, protein synthesis, and stress tolerance in plants [30]. The statistical analysis of the data was adjusted to normal distribution. Seed germination and elongation (root and hypocotyl) of *Lactuca sativa* are influenced by the contact with nanZnO. The results obtained when 10 mg/L of tartrazine solution, and aqueous solution treated by the adsorption- photocatalysis coupled process and diluted (100, 75, 50, 25 and 12.5%) were left with seeds of *Lactuca sativa* for 120 hours are shown in Figs. 8 and 9, the results were compared with the control (-).

The results show a decrease in hypocotyl and root growth of the "*Lactuca sativa*" that was put in contact with the nanoparticle. There were no significant differences for all treatments (10 mg / L of tartrazine solution, treated and diluted aqueous solution (100, 75, 50, 25 and 12.5%) except for the nanZnO exposure ($p < 0.05$) compared with the control (-).

Similar results were obtained for ZnO engineered nanoparticles (500 - 1500 mg/L) on the growth of *Brassica juncea* which might be due to the dose and tolerability of the plant species [31]. Therefore, the toxicity of nanZnO depends on the extent of dissolved Zn that is bioavailable to plants [30]. The toxicity of nanZn and nano-ZnO has been reported for different plants, such as radish, rape, ryegrass, lettuce, corn, and cucumber, a significant

inhibition of seed germination and an inhibition of root growth of most plants were observed, resulting in a decrease in the biomass [18].

All data were statistically analyzed by one-way ANOVA with post-hoc Dunnett test. It can be observed that with the remaining aqueous solution without dilution (100%), there is not any significant difference in the growth of radicle and hypocotyl with respect to the control (-), which indicates that the treatment decreases the sensitivity of the "*Lactuca sativa"* to the contaminant.

Fig. 9 shows the growth of plants (%) with respect to the control (-). It can be observed that the initial 10 mg/L tartrazine solution showed a grow increase of 20% in comparison to the control (-) and in both radicle and hypocotyl growth inhibition was observed when the seeds were in contact with nanZnO.

In addition, it was found that the majority of the samples that contained the highest amount of the dye in solution showed a stimulation on the growth of hypocotyl and radicle, this is a phytotoxic effect known as hormesis [21]. Some organic compounds (antibiotics) such as tetracycline and norfloxacin at 0.01 mg/L exhibited hormesis (growth of different plants) [32].

An study on the effect of ZnO nanoparticles on wheat plant (*Triticum aestivum*) in hydroponics media shows that ZnO nanoparticles in concentrations between 50 and 100 mg/L have positive effect on seed germination, roots and biomass in comparison with the negative control (distilled water) [33].

In contrast, a study reported that ZnO nanoparticles have more toxic effects on bread wheat and rye than ethylenediamine disuccinic acid (EDDS), while barley is positively affected by ZnO nanoparticles and EDDS. This behavior can be contradictory and therefore the

effects of ZnO nanoparticles varied depending on plants species and other factors, such as concentration, size, etc. [34].

Table 1 shows the toxicity indices of nanZnO in solution, the distributions of toxicity indices for RE are different, RE shows a great variability from -0.45 to -0.06 which indicates that they are sensible to the composition of the pollutant and SG varies from -0.26 to 0.12. The individual toxicity indices for SG and RE show that the toxicity is higher in root than in hypocotyl. These indices are designed in such a way that their values can vary from −1 > 0. In addition, if there is a 50% reduction in the variables studied (SG or RE) in relation to the control (-), this is considered as chronic toxicity, the term chronic is used to the long-term influence of these pollutants on the environment. The results did not show SG and RE elongation, the percentages were lower than 50% for both radicle and hypocotyl. Bagur-González et al. [21] established a phytotoxicity scale: 0 to −0.25 low toxicity, −0.25 to −0.5 moderate toxicity, −0.5 to −0.75 high toxicity and −0.75 to −1 very high toxicity and values >0 would indicate stimulation of the growth of the seed (hormesis). The results suggest that the "*Lactuca sativa*" species is suffering "low toxicity" when they are in contact with the solutions containing the dye and the remaining and diluted aqueous solutions (75 - 12.5 %) and the values obtained from the nanZnO and the remaining aqueous solution (100%) with the "*Lactuca sativa*" samples showed a growth inhibition in the seeds and a moderate index of toxicity.

ZnO nanoparticles added to natural soils can cause damage to germination, growth and alter the content of photosynthetic pigments due to the influence of soil pH, since in an acidic environments, the metals are more soluble and the entry of metals through the root and movement through the shoots is easier [35].

4. Conclusions

NanZnO and Ze-nanZnO were used for the removal of tartrazine from aqueous solutions by an adsorption-photocatalysis coupled process.

The tartrazine adsorption kinetics shows that the process is faster by using nanZnO than the composite Ze-nanZnO. The degradation of tartrazine in the adsorption-photocatalysis coupled process is efficient, 87 and 81% degradation were observed for nanZnO and Ze-nanZnO respectively, it is important to note that nanZnO is difficult to remove from the aqueous solution after the process. The mineralization of the dye was determined by analyzing the total organic carbon and it was between 85 and 90 %.

NanZnO affects "*Lactuca sativa*" species, the results indicate that the material produces "low toxicity" to this species.

Acknowledgements

This study received financial support from Conacyt (project 254665) and scholarship Grant No. 303739 for AAC.

References

[1] L. Bulgariu, L.B. Escudero, O.S. Bello, M. Iqbal, J. Nisar, K.A. Adegoke, F. Alakhras, M. Kornaros, I. Anastopoulos, The utilization of leaf-based adsorbents for dyes removal: A review, J. Mol. Liq. 276 (2019) 728–747.

[2] S.M. Prabhu, A. Khan, M. Hasmath Farzana, G.C. Hwang, W. Lee, G. Lee, Synthesis and characterization of graphene oxide-doped nano-hydroxyapatite and its adsorption performance of toxic diazo dyes from aqueous solution, J. Mol. Liq. 269 (2018) 746–754.

[3] I.K. Konstantinou, T.A. Albanis, TiO2-assisted photocatalytic degradation of azo dyes in aqueous solution: Kinetic and mechanistic investigations: A review, Appl. Catal. B Environ. 49 (2004) 1–14.

[4] J. Sokolowska-Gajda, H.S. Freeman, A. Reife, Synthetic Dyes Based on Environmental Considerations. Part 2: Iron Complexed Formazan Dyes*, 30 (1996) 1–20.

[5] M. Wawrzkiewicz, Z. Hubicki, Removal of tartrazine from aqueous solutions by strongly basic polystyrene anion exchange resins, J. Hazard. Mater. J. 164 (2009) 502–509.

[6] S. Banerjee, M.C. Chattopadhyaya, Adsorption characteristics for the removal of a toxic dye, tartrazine from aqueous solutions by a low cost agricultural by-product, Arab. J. Chem. 10 (2017) S1629–S1638.

[7] J. Liu, N. Wang, H. Zhang, J. Baeyens, Adsorption of Congo red dye on Fe x Co 3-x O 4 nanoparticles, J. Environ. Manage. 238 (2019) 473–483.

[8] R.I. Yousef, B. El-Eswed, A.H. Al-Muhtaseb, Adsorption characteristics of natural zeolites as solid adsorbents for phenol removal from aqueous solutions: Kinetics, mechanism, and thermodynamics studies, Chem. Eng. J. 171 (2011) 1143–1149.

[9] A. Nezamzadeh-Ejhieh, F. Khodabakhshi-Chermahini, Incorporated ZnO onto nano clinoptilolite particles as the active centers in the photodegradation of phenylhydrazine, J. Ind. Eng. Chem. 20 (2014) 695–704.

[10] Wang G, Liu S, He T, Liu X, Deng Q, Mao Y, Wang S, Enhanced visible-light-driven photocatalytic activities of Bi2Fe4O9/g-C3N4 composite photocatalysts, Mater. Res. Bull. 104 (2018) 104–111.

[11] C. Bojer, J. Schöbel, T. Martin, T. Lunkenbein, D. R. Wagner, A. Greiner, J. Breu, H.

Schmalz, Mesostructured ZnO/Au nanoparticle composites with enhanced photocatalytic activity, 128 (2017) 65-70.

[12] R. Nagaraja, N. Kottam, C.R. Girija, B.M. Nagabhushana, Photocatalytic degradation of Rhodamine B dye under UV/solar light using ZnO nanopowder synthesized by solution combustion route, Powder Technol. 215–216 (2012) 91–97.

[13] N. Mohaghegh, M. Tasviri, E. Rahimi, M.R. Gholami, Nano sized ZnO composites: Preparation, characterization and application as photocatalysts for degradation of AB92 azo dye, Mater. Sci. Semicond. Process. 21 (2014) 167–179.

[14] S. Danwittayakul, M. Jaisai, J. Dutta, Efficient solar photocatalytic degradation of textile wastewater using ZnO/ZTO composites, Appl. Catal. B Environ. 163 (2015) 1–

[15] H. Ma, P.L. Williams, S.A. Diamond, Ecotoxicity of manufactured ZnO nanoparticles - A review, Environ. Pollut. 172 (2013) 76–85.

[16] J.A. Hernandez-Viezcas, H. Castillo-Michel, A.D. Servin, J.R. Peralta-Videa, J.L. Gardea-Torresdey, Spectroscopic verification of zinc absorption and distribution in the desert plant Prosopis juliflora-velutina (velvet mesquite) treated with ZnO nanoparticles, Chem. Eng. J. 170 (2011) 346–352.

[17] L.R. Pokhrel, B. Dubey, Evaluation of developmental responses of two crop plants exposed to silver and zinc oxide nanoparticles, Sci. Total Environ. 452–453 (2013) 321–332.

[18] D. Lin, B. Xing, Phytotoxicity of nanoparticles: Inhibition of seed germination and root growth, Environ. Pollut. 150 (2007) 243–250.

[19]. A. Alcantara-Cobos, M. Solache-Ríos, E. Gutiérrez-Segura, Nobel materials (ZnO nanoparticles and ZnO nanoparticles supported on a zeolite) for the removal of tartrazine from aqueous solutions, Water, Air & Soil Pollut. (2019) 230:199.

[20] USEPA, Ecological Effects Test Guidline, United States Environ. Prot. Agency . (1996) 1–11.

[21] M.G. Bagur-González, C. Estepa-Molina, F. Martín-Peinado, S. Morales-Ruano, Toxicity assessment using Lactuca sativa L. bioassay of the metal(loid)s As, Cu, Mn, Pb and Zn in soluble-in-water saturated soil extracts from an abandoned mining site, J. Soils Sediments. 11 (2011) 281–289.

[22] B. Burger, K. Haas-Santo, M. Hunger, and J. Weitkamp, Synthesis and characterization of aluminium-rich zeolite ZSM-5. Chem. Eng. Technol. 23 (2000) 322–324.

[23] S. Moghaddasi, A. Fotovat, A.H. Khoshgoftarmanesh, F. Karimzadeh, H.R. Khazaei, R. Khorassani, Bioavailability of coated and uncoated ZnO nanoparticles to cucumber in soil with or without organic matter, Ecotoxicol. Environ. Saf. 144 (2017) 543–551.

[24] M. Khatamian, B. Divband, A. Jodaei, Degradation of 4-nitrophenol (4-NP) using ZnO nanoparticles supported on zeolites and modeling of experimental results by artificial neural networks, Mater. Chem. Phys. 134 (2012) 31–37.

[25] R. Javed, M. Usman, B. Yücesan, M. Zia, E. Gürel, Effect of zinc oxide (ZnO) nanoparticles on physiology and steviol glycosides production in micropropagated shoots of Stevia rebaudiana Bertoni, Plant Physiol. Biochem. 110 (2017) 94–99.

[26] S.M. Lam, J.C. Sin, I. Satoshi, A.Z. Abdullah, A.R. Mohamed, Enhanced sunlight photocatalytic performance over Nb2O 5/ZnO nanorod composites and the mechanism study, Appl. Catal. A Gen. 471 (2014) 126–135.

[27] A.A. Alswata, M. Bin Ahmad, N.M. Al-Hada, H.M. Kamari, M.Z. Bin Hussein, N.A. Ibrahim, Preparation of Zeolite/Zinc Oxide Nanocomposites for toxic metals removal from water, Results Phys. 7 (2017) 723–731.

[28] M.N. Zafar,Q. Dar, F. Nawaz, M.N. Zafar, M. Iqbal, M.F. Nazar, Effective adsorptive

removal of azo dyes over spherical ZnO nanoparticles, J. Mater. Res. Technol. (2018) 1–13.

[29] M. Leulescu, A. Rotaru, I. Pălărie, A. Moanţă, N. Cioateră, M. Popescu, E. Morîntale, M.V. Bubulică, G. Florian, A. Hărăbor, P. Rotaru, Tartrazine: physical, thermal and biophysical properties of the most widely employed synthetic yellow food-colouring azo dye, J. Therm. Anal. Calorim. 134 (2018) 209–231.

[30] J. Singh, S. Kumar, A. Alok, S.K. Upadhyay, M. Rawat, D.C.W. Tsang, N. Bolan, K.H. Kim, The potential of green synthesized zinc oxide nanoparticles as nutrient source for plant growth, J. Clean. Prod. 214 (2019) 1061–1070.

[31] S. Rao, G.S. Shekhawat, Toxicity of ZnO engineered nanoparticles and evaluation of their effect on growth, metabolism and tissue specific accumulation in Brassica juncea, J. Environ. Chem. Eng. 2 (2014) 105–114.

[32] M. Pan, L.M. Chu, Phytotoxicity of veterinary antibiotics to seed germination and root elongation of crops, Ecotoxicol. Environ. Saf. 126 (2016) 228–237.

[33] A. Awasthi, S. Bansal, L.K. Jangir, G. Awasthi, K.K. Awasthi, K. Awasthi, Effect of ZnO Nanoparticles on Germination of Triticum aestivum Seeds, Macromol. Symp. 376 (2017) 1–5.

[34] Z.G. Doğaroğlu, A. Eren, M.F. Baran, Effects of ZnO Nanoparticles and Ethylenediamine- N , N ′-Disuccinic Acid on Seed Germination of Four Different Plants , Glob. Challenges. 3 (2019) 1800111.

[35] C. García-Gómez, A. Obrador, D. González, M. Babín, M.D. Fernández, Comparative study of the phytotoxicity of ZnO nanoparticles and Zn accumulation in nine crops grown in a calcareous soil and an acidic soil, Sci. Total Environ. 644 (2018) 770–780.

Table 1. Toxicity indices for *Lactuca sativa* bioassay.

Samples	SG	RE	Toxicity
Control (-)	0	0	-
Control (+)	-0.05	-0.10	low
nanZnO	-0.26	-0.45	moderate
100%	-0.05	-0.27	moderate
75%	-0.05	-0.20	low
50%	0.12	-0.19	low
25%	0.01	-0.06	low
12.5%	-0.01	-0.12	low

Figures and tables captions

Fig. 1. X-ray diffraction patterns of (a) nanZnO and (b) Ze-nanZnO composite (Cli=Clinoptilolite).

Fig. 2. SEM images (2 000X) of (a) nanZnO (b), nanZnO-tartrazine, (c) Ze-nanZnO, (d) Ze-nanZnO-tartrazine and (e) and (f) TEM images of nanZnO particles.

Fig. 3. (a) UV-Vis spectrum of Baker commercial ZnO, (b) UV-Vis spectrum of NanZnO, (c) Diffuse reflectance spectra of nanZnO as a function of wavelength, (d) Energy band gap of NanZnO and Ze-NanZnO composite calculated by Kubelka-Munk function.

Fig. 4. (a) IR spectrum of tartrazine, nanZnO and the nanZnO treated with tartrazine and (b) IR spectrum of tartrazine, Ze-nanZnO and Ze-nanZnO treated with tartrazine.

Fig. 5. UV–Vis spectra of tartrazine during the adsorption-photocatalytic dye degradation at different time intervals by using a) nanZnO and (b) Ze-nanZnO.

Fig. 6. Concentration of tartrazine during the adsorption-photocatalytic degradation by (a) nanZnO and (b) Ze-nanZnO.

Fig. 7. TOC abatement by the adsorption-photocatalytic process as a function of time for the mineralization of tartrazine by using nanZnO (a) or Ze-nanZnO (b).

Fig. 8. Mean elongation ± SE (root and hypocotyl) of *Lactuca sativa* for the eight solutions (*indicates significance at the $p < 0.05$ level compared to the negative controls).

Fig. 9. Percentages of root and hypocotyl elongations.

Table 1. Elemental analysis of the nanZnO and Ze-nanZnO before and after tartrazine removal by EDS.

Table 2. Toxicity indices for *Lactuca sativa* bioassay.

Figures

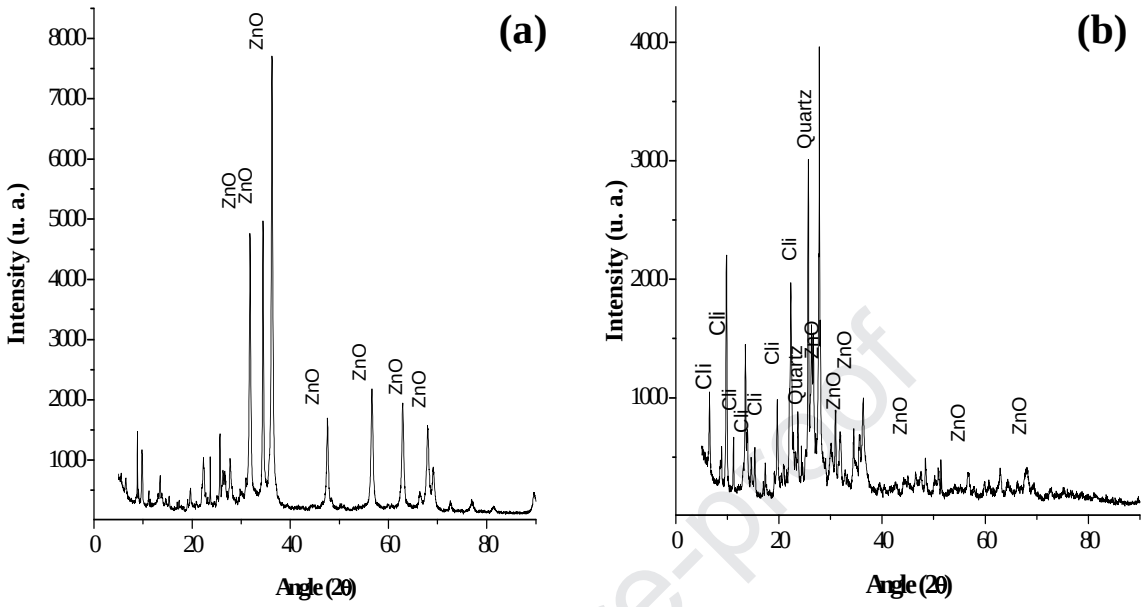

Fig. 1.

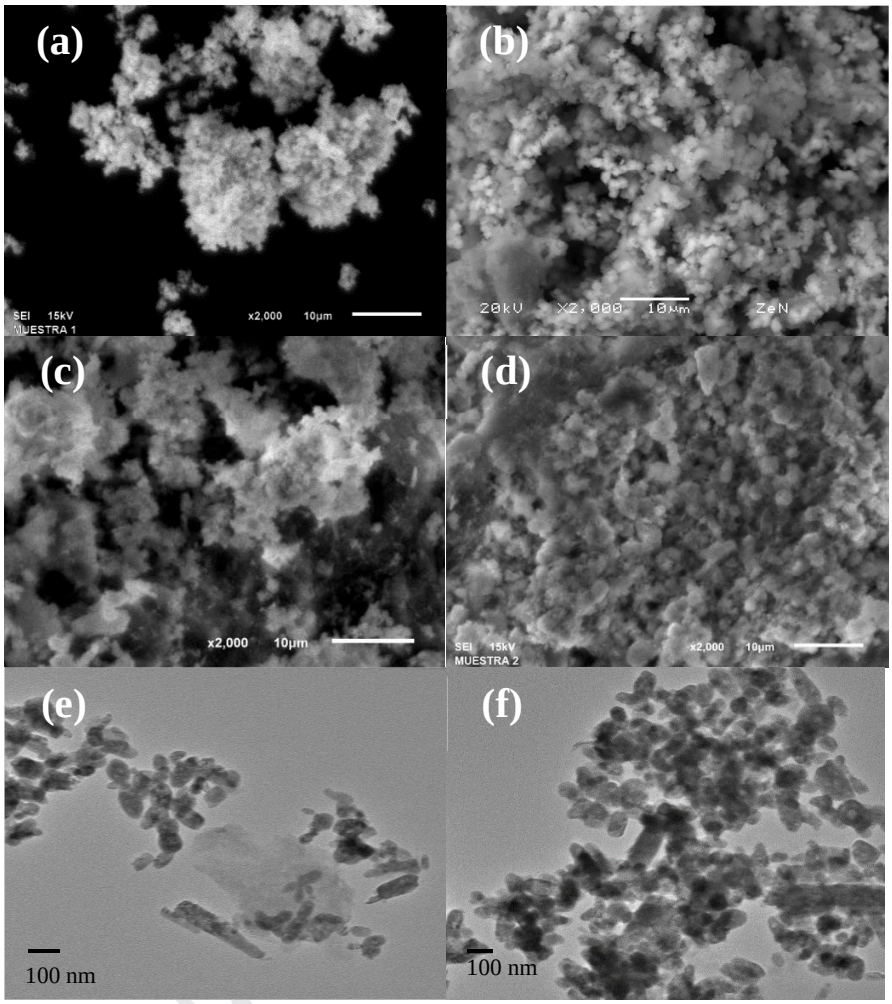
(a)
SEI 15kV
MUESTRA 1
x2,000 10µm
(b)
20kV X2,000 10µm ZeN
(c)
x2,000 10µm
(d)
SEI 15kV
MUESTRA 2
x2,000 10µm
(e)
100 nm
(f)
100 nm

Fig. 2.

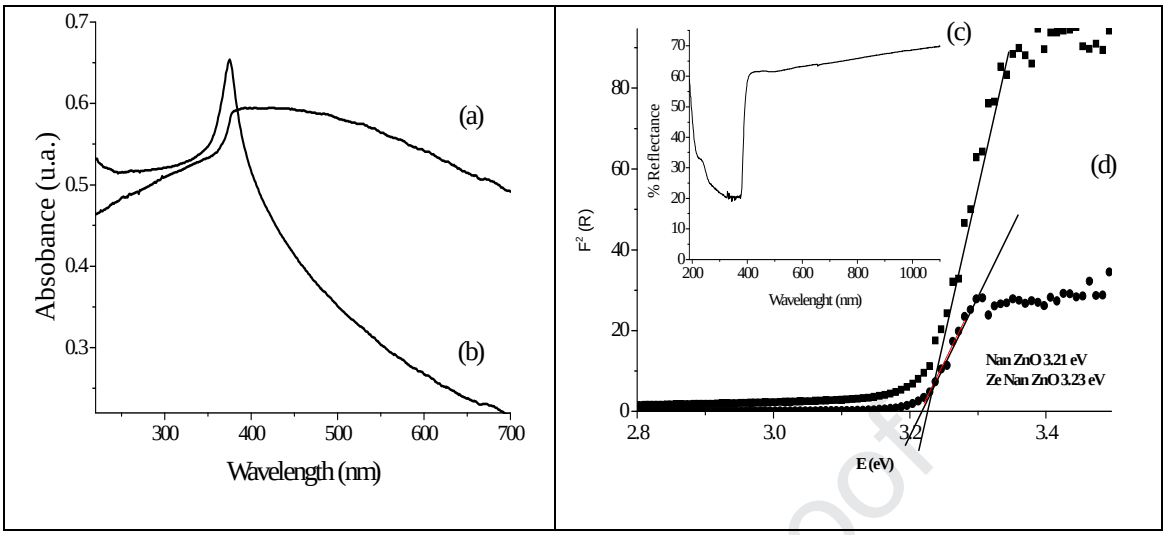
Absobance (u.a.)
Wavelength (nm)
(a)
(b)
(c)
(d)
% Reflectance
Wavelenght (nm)
F² (R)
E (eV)
Nan ZnO 3.21 eV
Ze Nan ZnO 3.23 eV

Fig. 3.

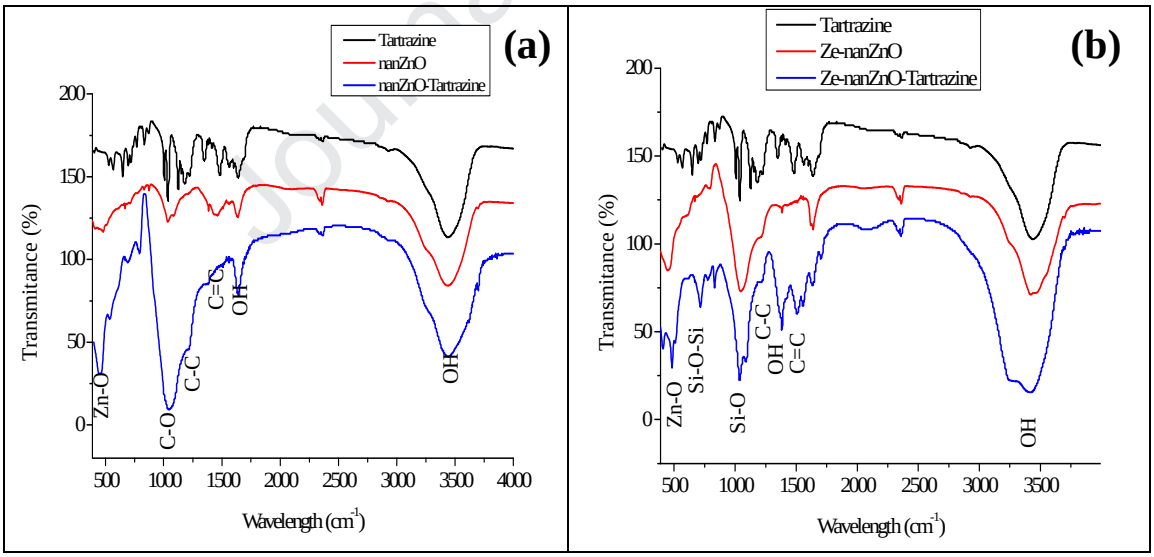
Tartrazine
nanZnO
nanZnO-Tartrazine
(a)
Transmitance (%)
Wavelength (cm⁻¹)
Zn-O
C-O
C-C
C=C
OH
Tartrazine
Ze-nanZnO
Ze-nanZnO-Tartrazine
(b)
Si-O-Si
Si-O

Fig. 4.

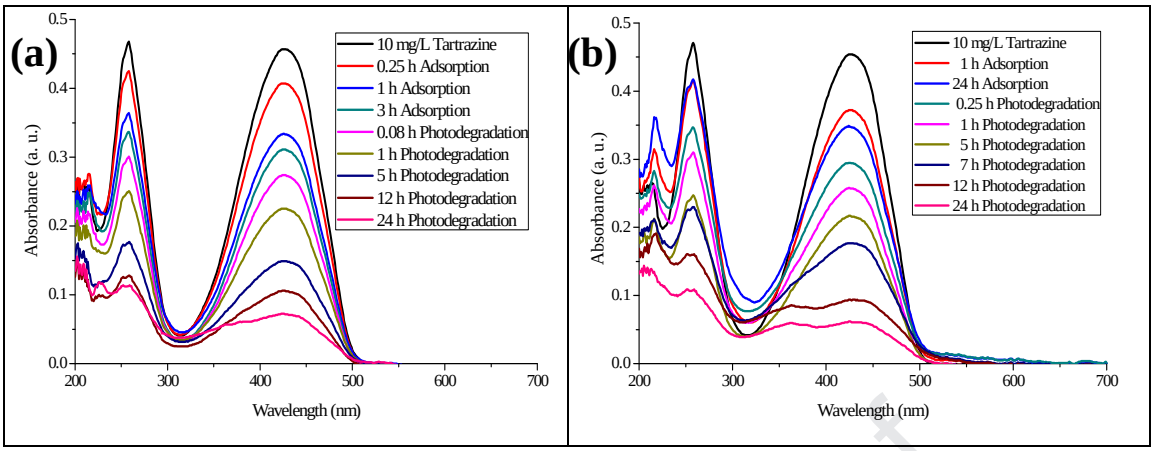

Fig. 5.

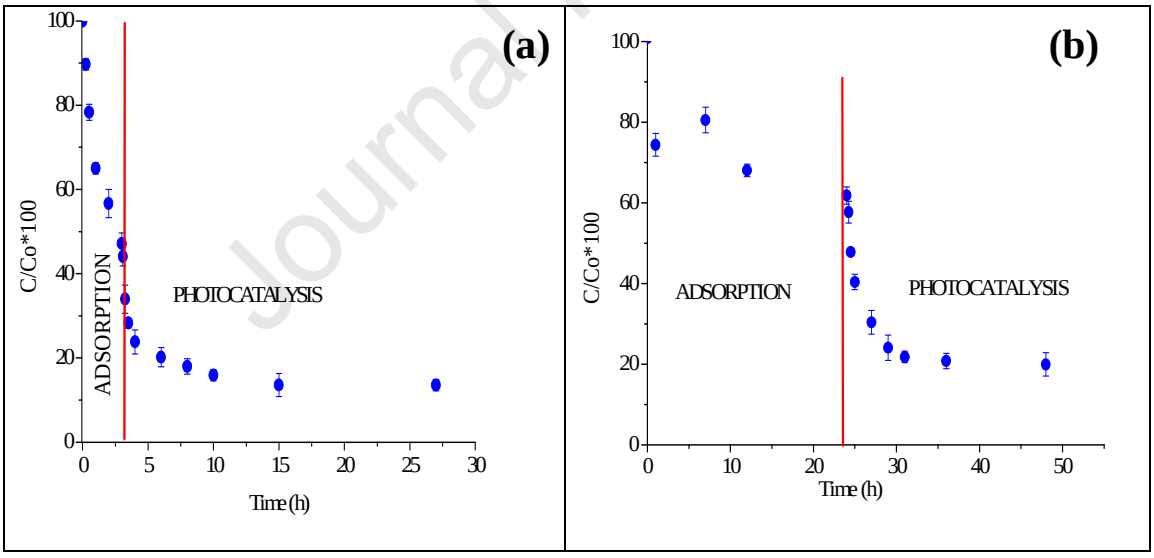

Fig. 6.

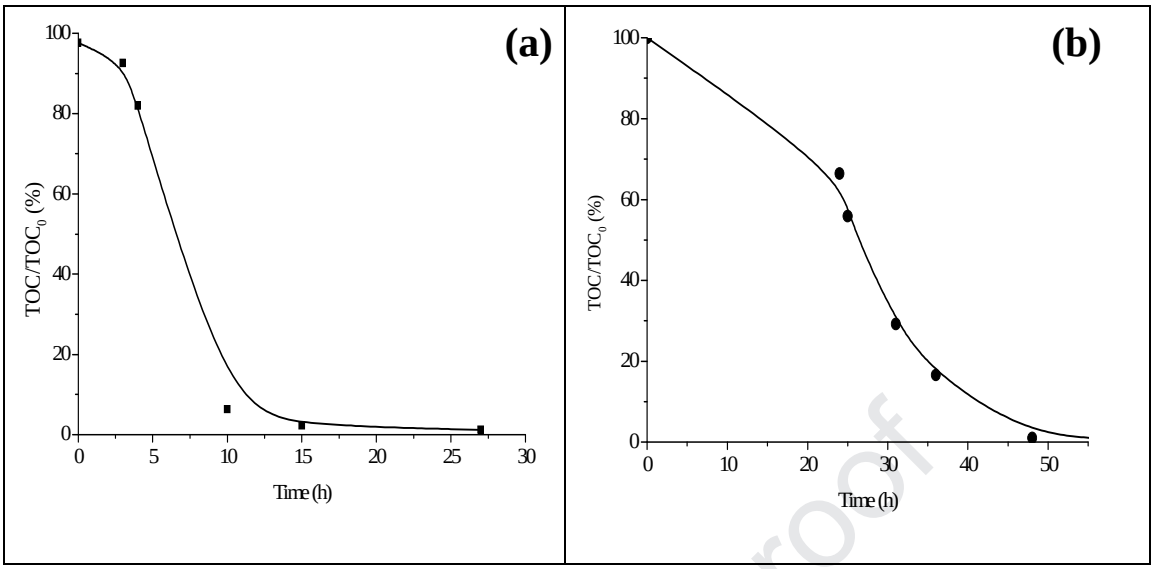
(a)
(b)
TOC/TOC0 (%)
Time (h)

Fig. 7.

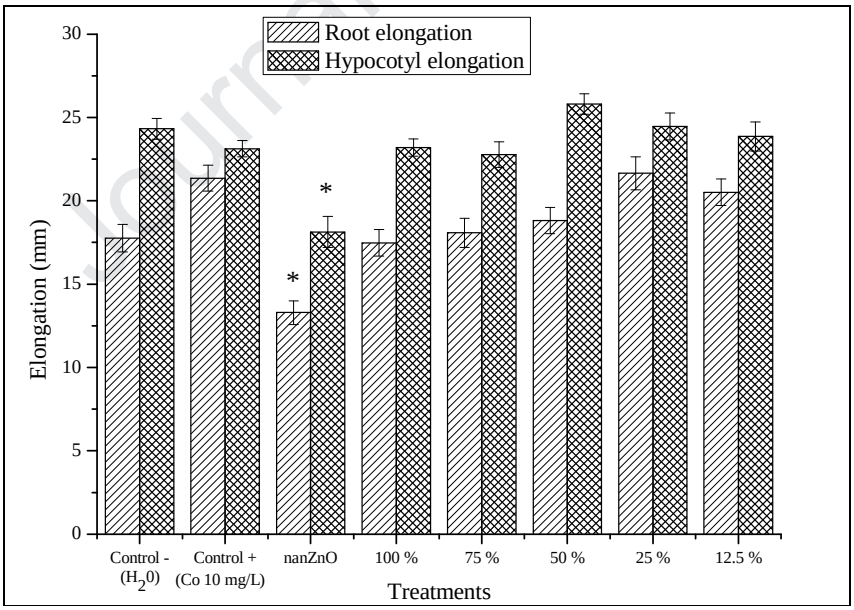
Root elongation
Hypocotyl elongation
Elongation (mm)
Control - (H2O)
Control + (Co 10 mg/L)
nanZnO
100 %
75 %
50 %
25 %
12.5 %
Treatments

Fig. 8.

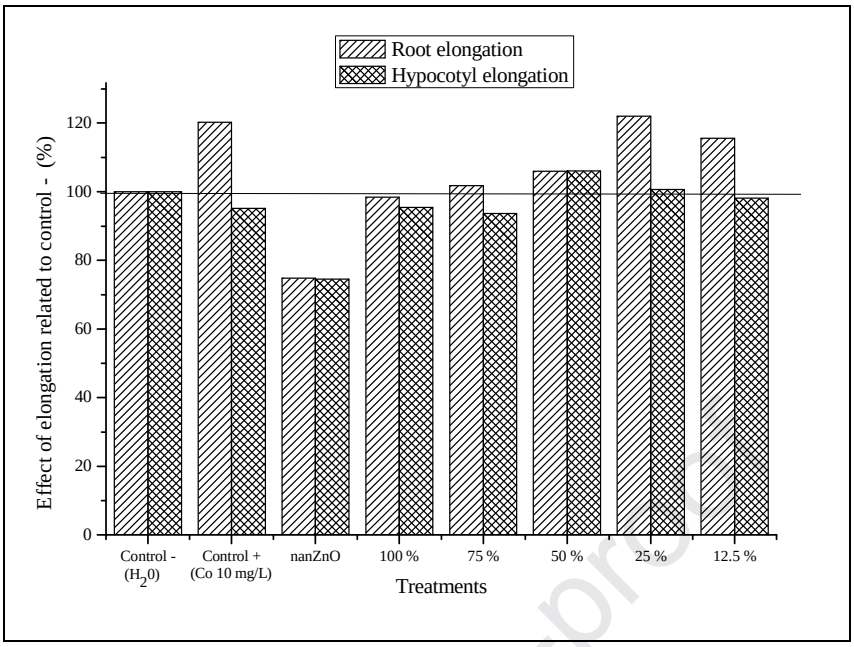

Fig. 9.

Highlights

- Tartrazine was removed from aqueous solutions by an adsorption-photocatalysis coupled process.
- Degradation of tartrazine by both materials in the presence of ultraviolet light is efficient.
- The degradation of the dye was high between 85 and 90 %.
- "Lactuca sativa" species suffer "low toxicity" when in contact with nanZnO

Declaration of interests

☒ The authors declare that they have no known competing financial interests or personal relationships that could have appeared to influence the work reported in this paper.

☐The authors declare the following financial interests/personal relationships which may be considered as potential competing interests:

'Declarations of interest: none'